Inorganic Chemistry

Article

pubs.acs.org/IC

Photoluminescent and Magnetic Properties of Lanthanide Containing Apatites: $Na_xLn_{10-x}(SiO_4)_6O_{2-y}F_y$, $Ca_xLn_{10-x}(SiO_4)_6O_{2-y}F_y$ (Ln = Eu, Gd, and Sm), $Gd_{9.34}(SiO_4)_6O_2$, and $K_{1.32}Pr_{8.68}(SiO_4)_6O_{1.36}F_{0.64}$

Allison M. Latshaw, Kendall D. Hughey, Mark D. Smith, Jeongho Yeon, and Hans-Conrad zur Loye*

Department of Chemistry and Biochemistry, University of South Carolina, Columbia, South Carolina 29208, United States

Supporting Information

ABSTRACT: Single crystals of $NaEu_9(SiO_4)_6O_2$, $Na_{1.5}Eu_{8.5}(SiO_4)_6OF$, $Na_{1.64}Gd_{8.36}(SiO_4)_6O_{0.72}F_{1.28}$, $Gd_{9.34}(SiO_4)_6O_2$, $Ca_{2.6}Eu_{7.4}(SiO_4)_6O_{1.4}F_{0.6}$, $Ca_{4.02}Sm_{5.98}(SiO_4)_6F_2$, and $K_{1.32}Pr_{8.68}(SiO_4)_6O_{1.36}F_{0.64}$ and powders of $NaEu_9(SiO_4)_6O_2$, $Na_{1.5}Eu_{8.5}(SiO_4)_6OF$, $Eu_{9.34}(SiO_4)_6O_2$, and $Gd_{9.34}(SiO_4)_6O_2$ were synthesized via flux growth in selected alkali-fluoride melts. All of the compounds adopt the apatite structure with space group $P6_3/m$. Luminescence and magnetic data were collected on $NaEu_9(SiO_4)_6O_2$, $Na_{1.5}Eu_{8.5}(SiO_4)_6OF$, $Eu_{9.34}(SiO_4)_6O_2$, and $Gd_{9.34}(SiO_4)_6O_2$. Luminescent data indicate that changing the cations and anions that surround the lanthanide site does not change the luminescent properties, making apatites versatile structures for optical materials.

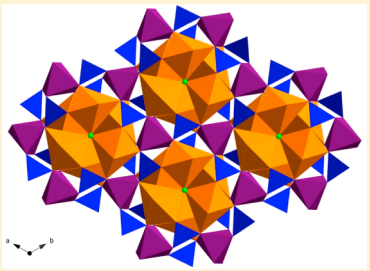

INTRODUCTION

Apatite structures have long been studied for many potential applications ranging from electrolytes for solid fuel cells[1] to solid state laser hosts[2] to phosphors used in luminescent devices.[3] More recently, the potential applications of materials belonging to this extensive structural family in solid state lighting have further increased interest in exploring the apatite structure and in preparing new rare earth containing compositions crystallizing in the apatite structure.

The apatite structure type is named after a class of minerals that have the composition $Ca_5(PO_4)_3X$, where X = F, Cl, or OH. The nomenclature within the apatite mineral class is extensive and overlapping. For this reason, we will apply the basic nomenclature when discussing apatite structures and use the X component to distinguish the apatites; specifically, we will refer to a fluoroapatite when X = F, a chlorapatite when X = Cl, a hydroxyapatite when X = OH, and an oxyapatite when X = O.[4]

Within the extensive family of known apatites, many are reported using the composition $A_{10}(BO_4)_6X_2$, instead of $A_5(BO_4)_3X$. This doubled composition is helpful when sites A and X are occupied by two different cations or anions, as reported herein. In general, "apatite" is used to describe a material with the composition $A_{10}(BO_4)_6X_2$, where A is a large cation, such as an alkali, alkaline-earth, or lanthanide metal cation or a mix of two of these; B is a smaller cation, such as arsenic ($Sr_{10}(AsO_4)_6Cl_2$),[5] boron, chromium ($Sr_{10}(CrO_4)_6F_2$),[6] germanium ($NaLa_9(GeO_4)_6O_2$),[7] phosphorus, silicon ($Na_{0.5}Nd_{4.5}(SiO_4)_3O$),[8] sulfur, or vanadium ($Ba_5(VO_4)_3OH$);[9] and X is an anion, such as fluorine, chlorine, or oxygen, or a combination of two of these.[10] For the compositions reported herein it is best to think of the apatite composition as $AA'(BO_4)_6XY$, where A = Ca, K, or Na; A′ = Ln (Eu, Gd, or Sm); B = Si; and X and Y = O or F.

The silicate apatite structure can act as a sensitizer by absorbing UV radiation and transmitting it to an activator, making it a good host structure for luminescence, as noted in the review by Waychunas in 2002.[11] It was also noted in the review that despite this ability, the silicate apatite structure has rarely been studied for its luminescent properties.

In this paper, we are reporting on our efforts to synthesize new rare earth containing silica based apatite materials and on our investigation of the luminescent and magnetic properties observed in silicate apatites. Herein, we present the crystal structures of seven new apatite oxides and oxyfluorides, along with the photoluminescence and magnetic properties of $NaEu_9(SiO_4)_6O_2$, $Na_{1.5}Eu_{8.5}(SiO_4)_6OF$, $Eu_{9.34}(SiO_4)_6O_2$, and $Gd_{9.34}(SiO_4)_6O_2$. The luminescence study indicates that lanthanide containing silicate apatites display luminescent properties that are essentially not affected by other cations or anions, making them good candidates in the search for new optical materials.

EXPERIMENTAL SECTION

Materials Preparation. Eu_2O_3 (99.9%), Gd_2O_3 (99.9%), Sm_2O_3 (99.99%), Pr_2O_3 reduced from Pr_6O_{11} (99.9%), LiF (98+%), $CaCO_3$ (99.95%), $Na_2MoO_4{\cdot}2H_2O$ (99.5−103.0%), KF (99% min), and NaF (99% min) were purchased from Alfa Aesar. Na_2CO_3 was purchased from Fisher Scientific, KCl (99.42%) from Mallinckrodt, and SiO_2 (99.99%) was purchased from Aldrich as fused pieces and ground to a powder in a ball mill.

Sample Preparation. The conditions described for the crystal growth of the various compositions are those found empirically to give the best yield and crystal quality. A compilation of the flux crystal growth reactions is given in Table 1.

Special Issue: To Honor the Memory of Prof. John D. Corbett

Received: September 8, 2014
Published: November 5, 2014

   dx.doi.org/10.1021/ic502185b | Inorg. Chem. 2015, 54, 876−884

Table 1. Reaction Conditions of the Flux Crystal Growth Syntheses of the Titled Compounds

compound	reactants			flux	flux melting point	dwell temp. time	cooling temp. rate
$Na_{1.5}Eu_{8.5}(SiO_4)_6OF$	Eu_2O_3	Na_2CO_3	SiO_2	NaF	993 °C	1150 °C	1000 °C
	2 mmol	2 mmol	4 mmol			12 h	6 °C/h
$NaEu_9(SiO_4)_6O_2$	Eu_2O_3	Na_2CO_3	SiO_2	$NaF:Na_2MoO_4$	614 °C	750 °C	550 °C
	2 mmol	2 mmol	4 mmol			12 h	6 °C/h
$Na_{1.62}Gd_{8.36}(SiO_4)_6O_{0.72}F_{1.28}$	Gd_2O_3		SiO_2	$NaF:Na_2MoO_4$	614 °C	750 °C	550 °C
	1 mmol		2 mmol			12 h	6 °C/h
$Gd_{9.34}(SiO_4)_6O_2$	Gd_2O_3		SiO_2	KF:KCl	606 °C	750 °C	550 °C
	1 mmol		2 mmol			10 days	6 °C/h
$Ca_{2.6}Eu_{7.4}(SiO_4)_6O_{1.4}F_{0.6}$	Eu_2O_3	$CaCO_3$	SiO_2	KF:KCl	606 °C	750 °C	550 °C
	1 mmol	2 mmol	1 mmol			24 h	6 °C/h
$Ca_{4.02}Sm_{5.98}(SiO_4)_6F_2$	Sm_2O_3	$CaCO_3$	SiO_2	KF:KCl	606 °C	750 °C	550 °C
	1 mmol	2 mmol	1 mmol			24 h	6 °C/h
$K_{1.32}Pr_{8.68}(SiO_4)_6O_{1.36}F_{0.64}$	Pr_2O_3		SiO_2	KF	858 °C	1000 °C	800 °C
	2 mmol		4 mmol			24 h	6 °C/h

Single crystals of $Na_{1.5}Eu_{8.5}(SiO_4)_6OF$, $NaEu_9(SiO_4)_6O_2$, and $Na_{1.62}Gd_{8.36}(SiO_4)_6O_{0.72}F_{1.28}$ were grown out of a sodium fluoride flux. Crystals of $Na_{1.5}Eu_{8.5}(SiO_4)_6OF$ were prepared by loading a 2:2:4 mmol ratio of Eu_2O_3:Na_2CO_3:SiO_2 into a platinum crucible. A total of 5 g of NaF flux was placed on top of the reactants, and a platinum lid was loosely fitted onto the crucible. The crucible was placed into a programmable furnace that was heated to 1150 °C over 1.5 h, allowed to dwell there for 12 h, and then slow cooled at a rate of 6 °C per hour to 1000 °C, after which the furnace was shut off. The flux was washed away using water, aided by sonication, and then the crystals were isolated by filtration.

$NaEu_9(SiO_4)_6O_2$ crystals were prepared by loading a 2:2:4 mmol ratio of Eu_2O_3:Na_2CO_3:SiO_2 into a silver crucible. 3.37:3.11 g of $NaF:Na_2MoO_4$ flux was placed on top of the reactants, and a silver lid was loosely fitted onto the crucible. The crucible was placed into a programmable furnace that was heated to 750 °C over 1.5 h, allowed to dwell there for 12 h, and then slow cooled at a rate of 6 °C per hour to 550 °C, after which the furnace was shut off. The flux was washed away using water, aided by sonication, and then the crystals were isolated by filtration.

$Na_{1.62}Gd_{8.36}(SiO_4)_6(O_{0.72}F_{1.28})$ crystals were prepared by loading a 1:2 mmol ratio of Gd_2O_3:SiO_2 into a silver crucible. A 0.2519:4.95 g ratio of $NaF:Na_2MoO_4$ flux was placed on top of the reactants, and a silver lid was loosely fitted onto the crucible. The crucible was placed into a programmable furnace that was heated to 750 °C over 1.5 h, allowed to dwell there for 12 h, and then slow cooled at a rate of 6 °C per hour to 550 °C, after which the furnace was shut off. The flux was washed away using water, aided by sonication, and then the crystals were isolated by filtration.

Crystals of $Gd_{9.34}(SiO_4)_6O_2$ were prepared by loading a 1:2 mmol ratio of Gd_2O_3:SiO_2 into a silver crucible. A 1.86:2.97 g ratio of KF:KCl flux was placed on top of the reactants, and a silver lid was loosely fitted onto the crucible. The crucible was placed into a programmable furnace that was heated to 750 °C over 1.5 h, allowed to dwell there for 10 days, and then slow cooled at a rate of 6 °C per hour to 550 °C, after which the furnace was shut off. The flux was washed away using water, aided by sonication, and then the crystals were isolated by filtration.

Crystals of $Ca_{2.6}Eu_{7.4}(SiO_4)_6O_{1.4}F_{0.6}$ and $Ca_{4.02}Sm_{5.98}(SiO_4)_6F_2$ were prepared by loading a 2:1:1 mmol ratio of $CaCO_3$:SiO_2:Ln_2O_3 into a silver crucible. A 1.85:2.97 g ratio of KF:KCl flux was placed on top of the reactants, and a silver lid was loosely fitted onto the crucible. The crucible was placed into a programmable furnace that was heated to 750 °C over 1.5 h, allowed to dwell there for 24 h, and then slow cooled at a rate of 6 °C per hour to 550 °C, after which the furnace was shut off. The flux was washed away using water, aided by sonication, and then the crystals were isolated by filtration.

Crystals of $K_{1.32}Pr_{8.68}(SiO_4)_6O_{1.36}F_{0.64}$ were prepared by loading a 2:4 mmol ratio of Pr_2O_3:SiO_2 into a copper tube that was welded at one end. A total of 5 g of KF was then loaded on top of the reactants, and the top of the tube was crimped shut. The reaction was loaded into a flow-through furnace, which contained an outer quartz tube with N_2 gas flowing through it, an inner copper tube to prevent any flux leaks from shattering the outer quartz tube, and the reaction tube. The furnace was then programmed to heat to 1000 °C over 1.5 h and held there for 24 h before slow cooling to 800 °C at a rate of 6 °C per hour and then shutting off the furnace. The flux was washed away using water, aided by sonication, and then the crystals were isolated by filtration.

Polycrystalline samples of $NaEu_9(SiO_4)_6O_2$, $Gd_{9.34}(SiO_4)_6O_2$, and $Eu_{9.34}(SiO_4)_6O_2$ were also synthesized via a solid state route. For $NaEu_9(SiO_4)_6O_2$, a stoichiometric ratio of Na_2CO_3 (0.125 mmol), SiO_2 (1.5 mmol), and Eu_2O_3 (1.125 mmol) was ground for 30 min and then transferred to an alumina crucible. The reaction was then heated to 900 °C with multiple heating/grinding cycles before the temperature was increased to 950 °C with multiple heating/grinding cycles. For $Gd_{9.34}(SiO_4)_6O_2$ and $Eu_{9.34}(SiO_4)_6O_2$, stoichiometric ratios of Gd_2O_3 or Eu_2O_3 (1.1675 mmol) and SiO_2 (1.5 mmol) were ground for 30 min and then transferred to an alumina crucible. The reactions were then heated to 900 °C with multiple heating/grinding cycles before the temperature was increased to 950 °C, with regrinding occurring after 48 h of heating. No change took place between 900 and 950 °C; therefore, the temperature was increased to 1000 °C with multiple heating/grinding cycles before the temperature was increased to 1050 °C and reground after 48 h, followed by a final heat treatment at 1100 °C, with regrinding after 100 h.

A polycrystalline sample of $Na_{1.5}Eu_{8.5}(SiO_4)_6OF$ was also synthesized via a solid state route. A stoichiometric ratio of Eu_2O_3 (2.125 mmol), Na_2SiO_3 (0.125 mmol), SiO_2 (2.875 mmol), and NaF (0.5 mmol) was ground for 30 min and then pressed into a pellet. The pellet was then loaded into a small copper tube that was crimped at both ends to avoid losing fluoride. The copper tube was loaded into a flow-through furnace purged with N_2 gas. The reaction was heated to 850 °C, with regrinding occurring after 100 h of heating, before increasing the temperature to 900 °C, with multiple heating/grinding cycles until the pattern stopped changing.

Characterization. *Single Crystal X-ray Diffraction.* Single crystal X-ray diffraction data were collected on all titled compounds. X-ray intensity data from a colorless needle crystal of $NaEu_9(SiO_4)_6O_2$ and colorless hexagonal rod crystals of $Na_{1.5}Eu_{8.5}(SiO_4)_6OF$, $Gd_{9.34}(SiO_4)_6O_2$, $Na_{1.62}Gd_{8.36}(SiO_4)_6O_{0.72}F_{1.28}$, $Ca_{2.6}Eu_{7.4}(SiO_4)_6O_{1.4}F_{0.6}$, $Ca_{4.02}Sm_{5.98}(SiO_4)_6F_2$, and $K_{1.32}Pr_{8.68}(SiO_4)_6O_{1.36}F_{0.64}$ were collected using a Bruker SMART APEX diffractometer (Mo Kα radiation, λ = 0.71073 Å).[12] The data collection covered 100% of reciprocal space to $2\theta_{max}$ = 65.2°, 56.6°, 70.6°, 70.1°, 71.1°, 70.1°, and 56.58°, respectively, with R_{int} = 0.036, 0.025, 0.036, 0.040, 0.040, 0.052, and 0.031 after absorption correction. The raw area detector data frames were reduced and corrected for absorption effects using the SAINT+ and SADABS programs.[12] Final unit cell parameters were determined by least-squares refinement of reflections from the data set. The initial structural model was obtained by direct methods using SHELXS.[13] Subsequent difference Fourier

dx.doi.org/10.1021/ic502185b | Inorg. Chem. 2015, 54, 876−884

Table 2. Crystallographic Data for $NaEu_9(SiO_4)_6O_2$, $Na_{1.5}Eu_{8.5}(SiO_4)_6OF$, $Na_{1.64}Gd_{8.36}(SiO_4)_6O_{0.72}F_{1.28}$, $Gd_{9.34}(SiO_4)_6O_2$, $Ca_{4.02}Sm_{5.98}(SiO_4)_6F_2$, $Ca_{2.6}Eu_{7.4}(SiO_4)_6O_{1.4}F_{0.6}$, and $K_{1.32}Pr_{8.68}(SiO_4)_6O_{1.36}F_{0.64}$

formula	$NaEu_9(SiO_4)_6O_2$	$Na_{1.5}Eu_{8.5}(SiO_4)_6OF$	$Na_{1.64}Gd_{8.36}(SiO_4)_6O_{0.72}F_{1.28}$	$Gd_{9.34}(SiO_4)_6O_2$
fw	1975.18	1913.69	1940.02	2052.16
temp (K)	296(2)	296(2)	296(2)	296(2)
crystal syst	hexagonal	hexagonal	hexagonal	hexagonal
space group	$P6_3/m$	$P6_3/m$	$P6_3/m$	$P6_3/m$
a (Å)	9.4434(1)	9.4492(4)	9.4257(2)	9.4366(2)
c (Å)	6.9150(2)	6.9155(7)	6.8850(2)	6.9345(2)
V (Å^3)	534.047(19)	534.74(6)	529.74(3)	534.78(3)
Z	2	2	2	2
density (mg/m^3)	6.141	5.943	6.081	6.372
abs coeff (mm^{-1})	26.481	25.021	26.259	28.953
cryst size (mm^3)	0.12 × 0.04 × 0.04	0.09 × 0.04 × 0.04	0.08 × 0.06 × 0.04	0.10 × 0.06 × 0.05
2θ range (deg)	4.98−65.17	4.98−56.56	4.99−70.13	4.98−70.59
reflns collected	12296	7410	15179	14658
data/restraints/params	707/0/41	485/1/42	837/0/42	861/0/39
R (int)	0.0359	0.0250	0.0395	0.0360
GOF (F^2)	1.292	1.179	1.245	1.341
R indices (all data)	R_1 = 0.0228	R_1 = 0.0195	R_1 = 0.0265	R_1 = 0.0280
	wR_2 = 0.0482	wR_2 = 0.0409	wR_2 = 0.0562	wR_2 = 0.0646

formula	$Ca_{4.02}Sm_{5.98}(SiO_4)_6F_2$	$Ca_{2.6}Eu_{7.4}(SiO_4)_6O_{1.4}F_{0.6}$	$K_{1.32}Pr_{8.68}(SiO_4)_6O_{1.36}F_{0.64}$
fw	1650.98	1814.6	1861.17
temp (K)	296(2)	296(2)	294(2)
crystal syst	hexagonal	hexagonal	hexagonal
space group	$P6_3/m$	$P6_3/m$	$P6_3/m$
a (Å)	9.4792(6)	9.4515(2)	9.6103(2)
c (Å)	6.9358(8)	6.9181(3)	7.1367(2)
V (Å^3)	539.72(9)	535.20(3)	570.82(2)
Z	2	2	2
density (mg/m^3)	5.079	5.630	5.414
abs coeff (mm^{-1})	17.429	22.417	18.814
cryst size (mm^3)	0.12 × 0.04 × 0.03	0.12 × 0.03 × 0.02	0.24 × 0.12 × 0.10
2θ range (deg)	4.96−70.12	4.98−71.16	4.90−56.58
reflns collected	12616	14418	5979
data/restraints/params	849/0/42	879/0/43	510/0/42
R (int)	0.0516	0.0396	0.0310
GOF (F^2)	1.314	1.291	1.299
R indices (all data)	R_1 = 0.0483	R_1 = 0.0268	R_1 = 0.0152
	wR_2 = 0.0808	wR_2 = 0.0583	wR_2 = 0.0356

calculations and full-matrix least-squares refinement against F^2 were performed with SHELXL-2013/4[2], using the ShelXle interface.[14]

The compounds crystallize in the hexagonal space group $P6_3/m$, as determined by the pattern of systematic absences in the intensity data and by the structure solution. These compounds adopt the fluoroapatite ($Ca_5(PO_4)_3F$) structure type. The apatite structure contains two unique lanthanide sites, where Ln(1) is located on a 3-fold axis (Wyckoff symbol 4*f*, site symmetry 3), while Ln(2) is located on a mirror plane (site 6*h*, site symmetry m). In $NaEu_9(SiO_4)_6O_2$, sodium mixes on the Ln(1) site, while in $Na_{1.5}Eu_{8.5}(SiO_4)_6OF$, $Gd_{8.36}Na_{1.62}(SiO_4)_6O_{0.72}F_{1.28}$, $Ca_{2.6}Eu_{7.4}(SiO_4)_6O_{1.4}F_{0.6}$, $Ca_{4.02}Sm_{5.98}(SiO_4)_6F_2$, and $K_{1.32}Pr_{8.68}(SiO_4)_6O_{1.36}F_{0.64}$, sodium or potassium mixes on both the Ln(1) and Ln(2) sites. For $Gd_{9.34}(SiO_4)_6O_2$, there is a partial vacancy on the Ln(1) site that matches what has been previously reported for the $Gd_{9.34}(SiO_4)_6O_2$ compound.[15] Atoms Si(1), O(1), and O(2) are located on mirror planes (site 6*h*, site symmetry *m*). Oxygen O(3) is located on a general position (site 12*i*), and oxygen O(4) is located on site 2*a* with −6 site symmetry. Site 2*a* is occupied either by O(4), in $NaEu_9(SiO_4)_6O_2$ and $Gd_{9.34}(SiO_4)_6O_2$; a mixing of O(4) and F(1), in $Na_{1.5}Eu_{8.5}(SiO_4)_6OF$, $Gd_{8.36}Na_{1.62}(SiO_4)_6O_{0.72}F_{1.28}$, $Ca_{2.6}Eu_{7.4}(SiO_4)_6O_{1.4}F_{0.6}$, and $K_{1.32}Pr_{8.68}(SiO_4)_6O_{1.36}F_{0.64}$; or only F(1), in $Ca_{4.02}Sm_{5.98}(SiO_4)_6F_2$. All atoms were refined with anisotropic displacement parameters. Final atomic coordinates were standardized with Structure Tidy.[16−18]

Powder X-ray Diffraction. The powder X-ray diffraction patterns for the polycrystalline samples from the solid state reactions $NaEu_9(SiO_4)_6O_2$, $Na_{1.5}Eu_{8.5}(SiO_4)_6OF$, $Gd_{9.34}(SiO_4)_6O_2$, and $Eu_{9.34}(SiO_4)_6O_2$ were collected using a Rigaku Dmax/2100 powder diffractometer using Cu Kα radiation. Data for $NaEu_9(SiO_4)_6O_2$, $Na_{1.5}Eu_{8.5}(SiO_4)_6OF$, and $Gd_{9.34}(SiO_4)_6O_2$ were collected using a step scan covering the 2-theta range of 5−65° in steps of 0.02°. Data for the $Eu_{9.34}(SiO_4)_6O_2$ were collected using a step scan covering the 2-theta range of 5−120° in steps of 0.04°. PXRD patterns were collected on the compounds grown by flux growth; $Na_{1.64}Gd_{8.36}(SiO_4)_6O_{0.72}F_{1.28}$, $Gd_{9.34}(SiO_4)_6O_2$, $Ca_{2.6}Eu_{7.4}(SiO_4)_6O_{1.4}F_{0.6}$, $Ca_{4.02}Sm_{5.98}(SiO_4)_6F_2$, and $K_{1.32}Pr_{8.68}(SiO_4)_6O_{1.36}F_{0.64}$, all of which contain small amounts of unreacted, water insoluble SiO_2, Gd_2O_3 (about 5%), and CaF_2 (about 10−16%), as well as, in some cases, secondary phases like $K_3GdSi_2O_7$ (about 40%), $Eu(AlO_3)$ (about 33%), and another new praseodymium compound in the powder samples that cannot be removed by washing. Powder samples that included lanthanide containing secondary phases were not measured for luminescent properties because the impurities would affect the luminescence.

X-ray Photoelectron Spectroscopy. Survey and detailed scans of the polycrystalline sample of $Na_{1.5}Eu_{8.5}(SiO_4)_6OF$ were performed using X-

dx.doi.org/10.1021/ic502185b | Inorg. Chem. 2015, 54, 876−884

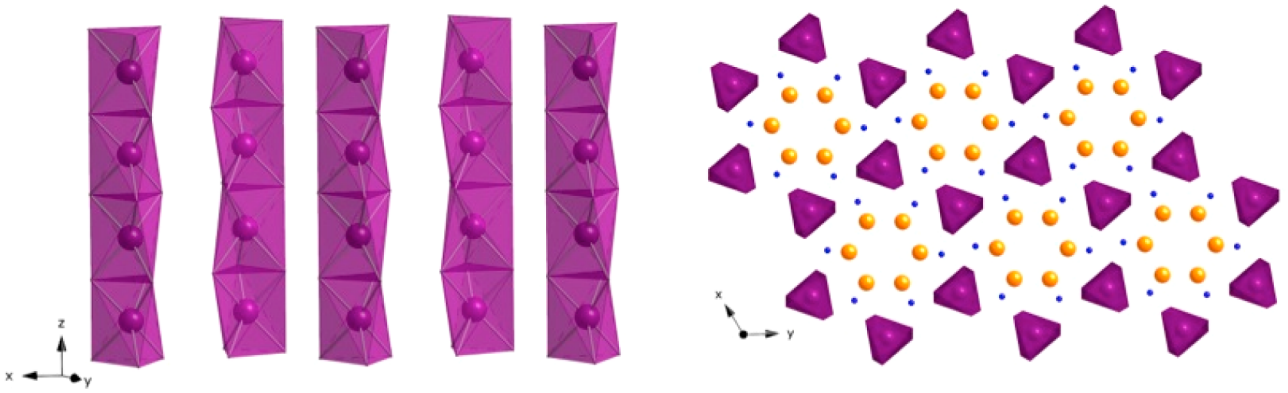

Figure 1. Crystal structure of $Na_{1.5}Eu_{8.5}(SiO_4)_6OF$, which is representative of the titled compounds. The left image represents the Ln(1) columns where the distortion of the columns can be seen, and the image on the right indicates the view of the Ln(1) columns shown down the *c* axis, where the purple polyhedra are the Ln(1) site, the orange spheres represent the Ln(2) site, and the blue spheres indicate the Si site.

ray Photoelectron Spectroscopy (XPS) on a Kratos AXIS Ultra DLD XPS system equipped with a monochromatic Al Kα. The Al Kα source had an operational level of 15 keV and 120 W, and the analyzer lens mode was hybrid. For the survey scan, the pass energy was fixed at 160 eV, the scan range was from 1350 eV to −0.8 eV, and the scan step was 400 meV with a dwell time of 500 ms. For the high-resolution XPS spectra acquisition, the pass energy was fixed at 40 eV; the scan range was chosen based on the interested elements, and the scan step was 60 meV with a dwell time of 2500 ms.

Luminescence. Emission and excitation spectra were collected on powders of $NaEu_9(SiO_4)_6O_2$, $Gd_{9.34}(SiO_4)_6O_2$, $Eu_{9.34}(SiO_4)_6O_2$, and $Na_{1.5}Eu_{8.5}(SiO_4)_6OF$ at room temperature using a PerkinElmer LS 55 fluorescence spectrometer. Excitation and emission scans were performed in the 225−500 and 550−900 nm ranges, respectively. Luminescence data of the other compounds were not collected due to the presence of lanthanide containing secondary phases that would have affected the data collection.

Magnetic Property Measurements. The DC magnetizations of $NaEu_9(SiO_4)_6O_2$, $Gd_{9.34}(SiO_4)_6O_2$, $Eu_{9.34}(SiO_4)_6O_2$, and $Na_{1.5}Eu_{8.5}(SiO_4)_6OF$ were measured as a function of temperature using a Quantum Design Magnetic Property Measurement System (QD-MPMS3 SQUID VSM). These compounds were placed in gel capsules. The samples were then cooled to 2 K under zero-field cooled (zfc) conditions. Data were collected from 2 to 300 K with an applied magnetic field of 1000 Oe. Corrections for the radial offset and sample shape were applied to the magnetism with a fitting routine that involved data collected at 30 K under both DC and VSM modes.[19] Magnetic properties of the other compounds were not collected due to the presence of lanthanide containing secondary phases that would have affected the sample magnetization.

RESULTS AND DISCUSSION

Powder X-ray Diffraction. The calculated and experimental PXRD patterns for the polycrystalline solid state reactions $NaEu_9(SiO_4)_6O_2$, $Na_{1.5}Eu_{8.5}(SiO_4)_6OF$, and $Gd_{9.34}(SiO_4)_6O_2$ are in excellent agreement, as seen in Figures S1−S3. $Eu_{9.34}(SiO_4)_6O_2$, which has been published previously as a polycrystalline powder,[20] was compared to $Gd_{9.34}(SiO_4)_6O_2$ (Figure S4). It was determined that there was a very small amount of Eu_2O_3 in the $Eu_{9.34}(SiO_4)_6O_2$ polycrystalline powder. The Eu_2O_3 can only been seen when zooming in on the powder pattern.

Crystal Structure. Alkali fluoride melts have been identified as good fluxes for the crystal growth of oxides[21] and were used to grow crystals of the title compounds. In order to lower the temperatures of the fluxes to carry out the reactions in silver instead of platinum crucibles, eutectic compositions were used. The fluxes used include NaF (mp 993°), NaF(34%)/NaCl(66%) (mp 679°), NaF(20%)/Na_2MoO_4(80%) (mp 614 °C), and KF(45%)/KCl(55%) (mp 606 °C). Crystal growth reactions carried out in the NaF and NaF containing eutectic fluxes consistently resulted in sodium incorporation into the reaction products, while reactions carried out in KF based eutectics did not result in the incorporation of potassium into the crystals. Only when KF was used neat did the potassium incorporate. All compounds crystallize in the hexagonal space group $P6_3/m$. The crystallographic data are compiled in Table 2.

Many of the known lanthanide silicate oxyapatites crystallize in the space group $P6_3/m$, as is the case for the title compounds; however, apatites are known to also crystallize in five other principle space groups including $P6_3$, $P\bar{3}$, $P\bar{6}$, $P2_1/m$, and $P2_1$.[3,10,22−31] All apatite structures contain columns consisting of distorted, face-sharing trigonal prisms as shown in Figure 1. In the case of apatites taking on the $P6_3/m$ space group, the Ln(1) site occupies the cation sites in these columns. As the space group changes to, for example, $P2_1/m$ or $P2_1$, either there are multiple cations occupying these columns or the distortions of the columns, called the metaprism twist angles, grow larger or less uniform. In the $P6_3/m$ space group, the metaprism twist angles must be uniform, while for space groups $P2_1/m$ and $P2_1$, there can be multiple metaprism angles for each trigonal prism.[22]

As observed previously in the literature, in compounds with the composition $A_xLn_{10-x}(SiO_4)_6O_2$, where A is an alkali or alkaline earth metal cation and Ln is a lanthanide, mixing of the A and Ln cations will only occur on the 4*f*, or Ln(1), site, leaving the 6*h*, or Ln(2), site fully occupied by the Ln cations. Compounds with compositions $A_xLn_{10-x}(SiO_4)_6OF$ or $A_xLn_{10-x}(SiO_4)_6F_2$, on the other hand, typically exhibit mixing of the A and Ln cations on both the 4*f* and 6*h* sites.[23] The 4*f* and 6*h* sites are shown in Figure 2.

In the $A_xLn_{10-x}(SiO_4)_6X_2$ apatite structure, there are two unique lanthanide polyhedra (Ln(1) and Ln(2)), an isolated SiO_4 tetrahedron and an O(4) site that contains either O^{2-}, F^-, or a mix of O^{2-} and F^-. Ln(1) is located in a six coordinated twisted trigonal prism. Ln(2) is located in a seven-coordinated distorted pentagonal bipyramid, and Si(1) is located in an isolated tetrahedron. Ln(1) and Ln(2) form columns down the *c* axis. The Ln(1) columns are formed by face-shared stacking of distorted trigonal prisms, as shown in Figure 1. The Ln(2) columns are formed when three Ln(2) polyhedra in each layer corner share through the O(4)/F(1) site to form $Ln(2)_3O_{19}$ units, as depicted in Figure 3. The $Ln(2)_3O_{19}$ units are rotated by 60° (Figure 3) to form the Ln(2) polyhedra columns down the *c*

dx.doi.org/10.1021/ic502185b | Inorg. Chem. 2015, 54, 876−884

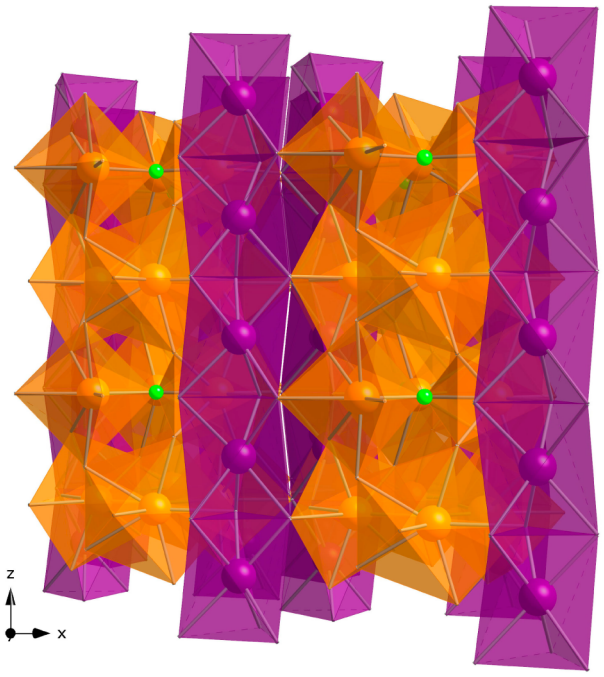

Figure 2. Crystal structure of $K_{1.32}Pr_{8.68}(SiO_4)_6O_{1.36}F_{0.64}$, which is representative of the titled compounds. The 4*f*, or Ln(1), site is shown as purple polyhedra. The 6*h* site is shown as orange polyhedra, and the O(4)/F(1) site is shown as green spheres.

axis (Figure 4). The lanthanide polyhedra are connected via edge sharing of the Ln(1) polyhedra with three of the Ln(2) columns. The isolated SiO_4 tetrahedra are located between the Ln(1) and Ln(2) containing columns. The overall view of the structure down the *c* axis is shown in Figure 5. In all of the compounds reported herein, the average Si−O bond distance is 1.62 Å, the average Ln(1)−O interatomic distance is 2.55 Å, and the average Ln(2)−O interatomic distance is 2.42 Å. Selected interatomic distances are tabulated in Table 3.

The metaprism twist angles of the Ln(1) polyhedra for the seven compounds range from 22.43 to 24.23°. These values fall into the range of twist angles of 5−25°, which is expected for apatites crystallizing in the $P6_3/m$ space group.[32]

X-ray Photoelectron Spectroscopy. The preparation of oxyfluoride samples via the solid-state route readily leads to the desired composition and structure. However, since it is very difficult to differentiate between oxygen and fluorine by X-ray diffraction, and because of the possibility that fluorine might be lost during the synthesis, X-ray photoelectron spectroscopy was used to confirm the presence of fluorine in a polycrystalline sample of $Na_{1.5}Eu_{8.5}(SiO_4)_6OF$. The survey scan in Figure 6 covered the entire sample surface and confirms the existence of Na, Eu, Si, O, and F elements. A high-resolution XPS spectrum covering the range of 705−670 eV revealed a peak at 685 eV (after a correction with C 1s, 284.6 eV), as shown in Figure 6, which conclusively indicates the presence of metal bound fluorine; it matches well with the metal bound F 1s peak range (684−685.8 eV) given in the Handbook of X-ray Photoelectron Spectroscopy.[33] These results confirm the presence of fluorine in the polycrystalline sample of $Na_{1.5}Eu_{8.5}(SiO_4)_6OF$ and its coordination nature.

Photoluminescence. Fluorescence data were collected on solid state powders of $NaEu_9(SiO_4)_6O_2$, $Na_{1.5}Eu_{8.5}(SiO_4)_6OF$, $Eu_{9.34}(SiO_4)_6O_2$, and $Gd_{9.34}(SiO_4)_6O_2$. The room temperature emission spectra for the europium containing compounds are shown in Figure 7, and the excitation spectra are shown in Figure 8. The emission spectra for the europium containing compounds were collected using an excitation wavelength of 230 nm, while the excitation spectra of the compounds were collected using an emission wavelength of 607 nm. The maximum emission peaks at 607 nm are typical for europium containing compounds.[34] In Figure 8, the excitation peaks of the europium containing compounds follow the expected set of peaks from 350 nm to 425 nm that indicate the transitions within the $4f^6$ configuration of the Eu^{3+} cation.

For the gadolinium compound, the excitation and emission spectra are displayed in Figure 9. The excitation wavelength was 250 nm, and the emission wavelength was 622 nm. The gadolinium compound exhibits excitation and emission spectra

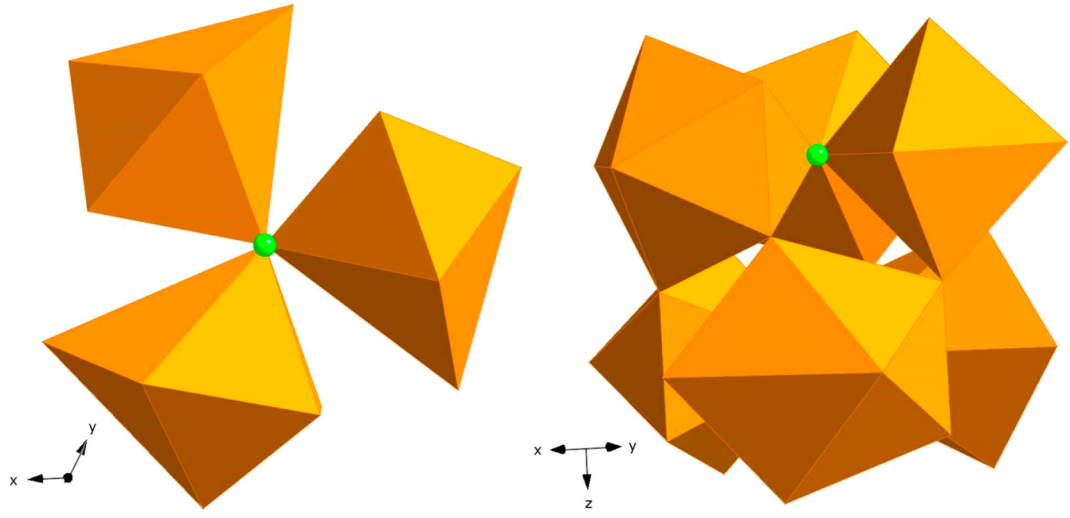

Figure 3. Crystal structure of $Na_{1.5}Eu_{8.5}(SiO_4)_6OF$, a representative structure of the title compounds. The $Ln(2)_3O_{19}$ or $Ln(2)_3O_{18}F$ group is shown on the left, where the orange polyhedra indicate each $Ln(2)O_7$ or $Ln(2)O_6F$ unit, and the green atom is the O(4) or F(1) site. The image on the left represents the 60° rotation that occurs for the $Ln(2)_3O_{19}$ units to form the columns down the *c* axis.

dx.doi.org/10.1021/ic502185b | *Inorg. Chem.* 2015, 54, 876−884

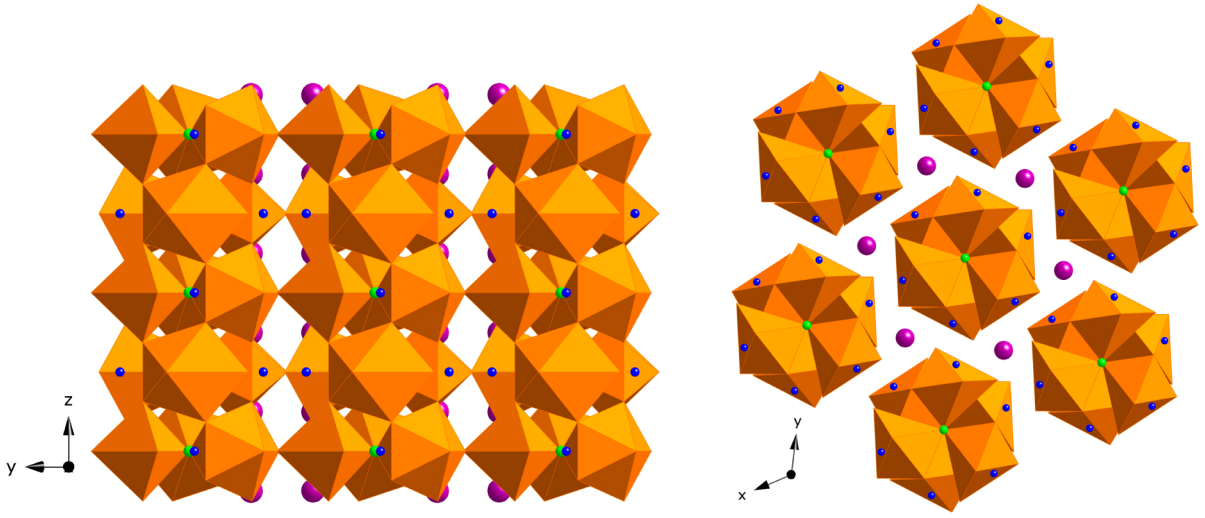

Figure 4. Crystal structure of $Na_{1.5}Eu_{8.5}(SiO_4)_6OF$, which is representative of the title compounds. The image on the left shows the stacking of the $Ln(2)_3O_{19}$ units down the *a* axis, and the image on the right is the view of the columns down the *c* axis. The orange polyhedra represent the Ln(2) site. The purple spheres represent the Ln(1) site. The blue spheres represent the Si site, and the green spheres represent the O(4)/F(1) site.

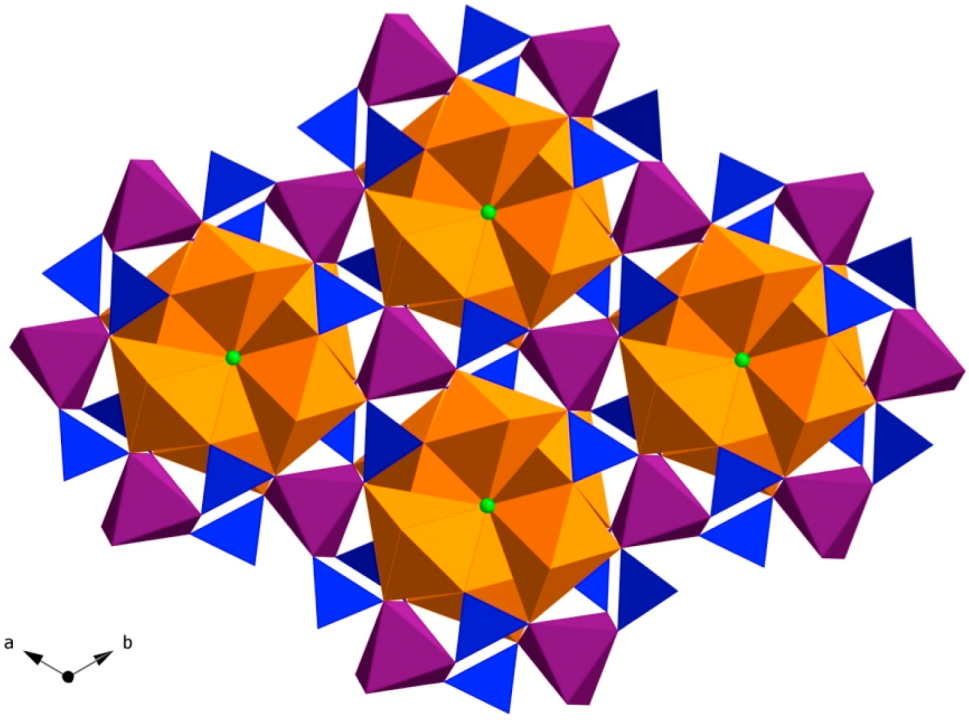

Figure 5. Crystal structure of $Na_{1.5}Eu_{8.5}(SiO_4)_6OF$, a representative structure of the title compounds down the *c* axis, where the Ln(1) polyhedra are shown in purple, Ln(2) polyhedra are shown in orange, SiO_4 tetrahedra are shown in blue, and the O(4)/F(1) site is shown in green.

peaks consistent with expected values for gadolinium containing compounds.

A close look at the luminescence data for $NaEu_9(SiO_4)_6O_2$, $Na_{1.5}Eu_{8.5}(SiO_4)_6OF$, and $Eu_{9.34}(SiO_4)_6O_2$ demonstrates that the excitation and emission data are almost identical. This suggests that changing the ratio of the cation atoms on the Ln sites and of the anion atoms on the X site does not change the luminescence. This result supports the hypothesis that doping other luminescent cations onto the lanthanide site will allow tuning of the luminescence.

Magnetic Properties. The temperature dependencies of the magnetic susceptibilities of $NaEu_9(SiO_4)_6O_2$, $Na_{1.5}Eu_{8.5}(SiO_4)_6OF$, $Eu_{9.34}(SiO_4)_6O_2$, and $Gd_{9.34}(SiO_4)_6O_2$ were measured over the temperature range of 2−300 K and are shown in Figures 10 and 11. The europium containing compounds display van Vleck paramagnetism, while the gadolinium compound follows the Curie−Weiss law. The effective moment at 300 K was determined for the three europium compounds, $NaEu_9(SiO_4)_6O_2$, $Eu_{9.34}(SiO_4)_6O_2$, and $Na_{1.5}Eu_{8.5}(SiO_4)_6OF$, and found to be 3.40, 3.42, and 3.18 μ_B/Eu, which compares well with the generally accepted 300 K value for Eu^{3+} of 3.4 μ_B/Eu. The $Gd_{9.34}(SiO_4)_6O_2$ susceptibility data collected from 2 to 300 K, when fit to the Curie−Weiss law, yielded an effective moment of 7.86 μ_B/Gd and a Weiss constant of θ = 0.3 K, which compares well to the expected value of 7.94 μ_B/Gd.

dx.doi.org/10.1021/ic502185b | *Inorg. Chem.* 2015, 54, 876−884

Table 3. Selected Bond Distances (in Å) for $NaEu_9(SiO_4)_6O_2$, $Na_{1.5}Eu_{8.5}(SiO_4)_6OF$, $Na_{1.64}Gd_{8.36}(SiO_4)_6O_{0.72}F_{1.28}$, $Gd_{9.34}(SiO_4)_6O_2$, $Ca_{4.02}Sm_{5.98}(SiO_4)_6F_2$, $Ca_{2.6}Eu_{7.4}(SiO_4)_6O_{1.4}F_{0.6}$, and $K_{1.32}Pr_{8.68}(SiO_4)_6O_{1.36}F_{0.64}$

	$NaEu_9(SiO_4)_6O_2$	$Na_{1.5}Eu_{8.5}(SiO_4)_6OF$	$Na_{1.64}Gd_{8.36}(SiO_4)_6O_{0.72}F_{1.28}$	$Gd_{9.34}(SiO_4)_6O_2$
Ln(1)−O(2) (×3)	2.382(3)	2.386(4)	2.373(3)	2.387(4)
Ln(1)−O(1) (×3)	2.456(3)	2.463(3)	2.449(3)	2.475(4)
Ln(1)−O(3) (×3)	2.813(4)	2.830(5)	2.803(4)	2.813(5)
Ln(2)−X[a]	2.2431(3)	2.2646(3)	2.2532(3)	2.2254(3)
Ln(2)−O(3) (×2)	2.336(3)	2.331(4)	2.317(3)	2.346(4)
Ln(2)−O(1)	2.405(4)	2.393(5)	2.382(4)	2.401(5)
Ln(2)−O(3) (×2)	2.489(4)	2.484(4)	2.479(4)	2.473(4)
Ln(1)−O(2)	2.664(5)	2.654(5)	2.662(5)	2.648(7)
	$Ca_{4.02}Sm_{5.98}(SiO_4)_6F_2$	$Ca_{2.6}Eu_{7.4}(SiO_4)_6O_{1.4}F_{0.6}$	$K_{1.32}Pr_{8.68}(SiO_4)_6O_{1.36}F_{0.64}$	
Ln(1)−O(2) (×3)	2.384(4)	2.377(3)	2.467(2)	
Ln(1)−O(1) (×3)	2.441(5)	2.443(3)	2.535(2)	
Ln(1)−O(3) (×3)	2.820(7)	2.799(4)	2.870(3)	
Ln(2)−X[a]	2.3287(6)	2.2465(3)	2.2814(2)	
Ln(2)−O(3) (×2)	2.325(5)	2.330(3)	2.429(3)	
Ln(2)−O(1)	3.386(7)	2.412(4)	2.462(3)	
Ln(2)−O(3) (×2)	2.505(5)	2.495(3)	2.550(2)	
Ln(1)−O(2)	2.680(8)	2.703(5)	2.684(4)	

[a]X = O(4) or F(1), respectively.

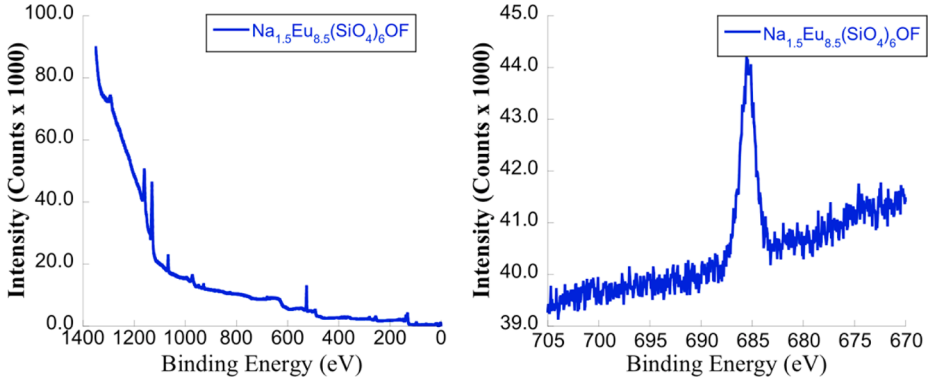

Figure 6. XPS data of $Na_{1.5}Eu_{8.5}(SiO_4)_6OF$. The image on the left depicts the survey scan that indicates the presence of Na, Eu, Si, O, and F, and the image on the right depicts the detailed scan of the region where the peak around 685 indicates the presence of metal fluoride bonding.

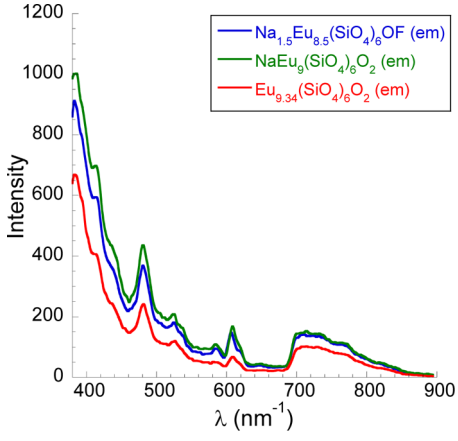

Figure 7. Emission spectra of $NaEu_9(SiO_4)_6O_2$, $Na_{1.5}Eu_{8.5}(SiO_4)_6OF$, and $Eu_{9.34}(SiO_4)_6O_2$.

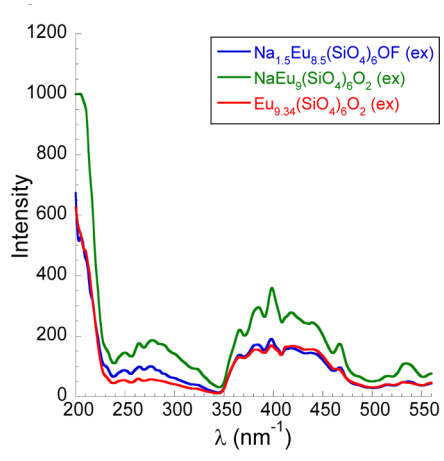

Figure 8. Excitation spectra of $NaEu_9(SiO_4)_6O_2$, $Na_{1.5}Eu_{8.5}(SiO_4)_6OF$, and $Eu_{9.34}(SiO_4)_6O_2$.

CONCLUSIONS

Single crystals of compounds of the apatite structure type, $NaEu_9(SiO_4)_6O_2$, $Na_{1.5}Eu_{8.5}(SiO_4)_6OF$, $Na_{1.64}Gd_{8.36}(SiO_4)_6O_{0.72}F_{1.28}$, $Gd_{9.34}(SiO_4)_6O_2$, $Ca_{2.6}Eu_{7.4}(SiO_4)_6O_{1.4}F_{0.6}$, $Ca_{4.02}Sm_{5.98}(SiO_4)_6F_2$, and $K_{1.32}Pr_{8.68}(SiO_4)_6O_{1.36}F_{0.64}$, were synthesized in fluoride fluxes, and $NaEu_9(SiO_4)_6O_2$, $Na_{1.5}Eu_{8.5}(SiO_4)_6OF$, $Eu_{9.34}(SiO_4)_6O_2$, and $Gd_{9.34}(SiO_4)_6O_2$ were prepared as polycrystalline powders

dx.doi.org/10.1021/ic502185b | Inorg. Chem. 2015, 54, 876−884

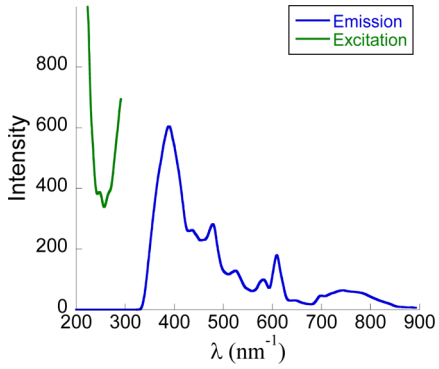

Figure 9. Emission and excitation spectra of $Gd_{9.34}(SiO_4)_6O_2$.

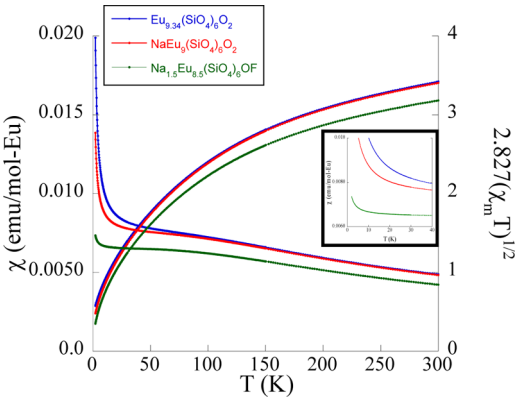

Figure 10. Temperature dependence of the magnetic susceptibility data and of the magnetic moments of $Eu_{9.34}(SiO_4)_6O_2$, $NaEu_9(SiO_4)_6O_2$, and $Na_{1.5}Eu_{8.5}(SiO_4)_6OF$.

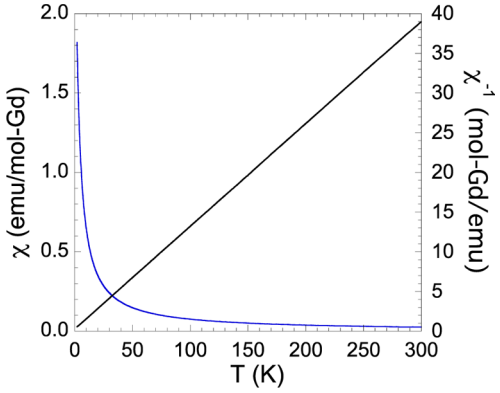

Figure 11. Temperature dependence of the magnetic susceptibility data and of the magnetic moment of $Gd_{9.34}(SiO_4)_6O_2$.

using solid state synthesis techniques. As previously reported, the mixing of the Ln(2) cation site is dependent upon substitution on the O(4) site with either F^- or OH^-. The luminescent properties of the silicon containing apatites indicate that these compounds may find potential applications in solid-state lighting, because the luminescence may be tunable.

■ ASSOCIATED CONTENT

Supporting Information

ICSD depository numbers for the titled compounds and powder X-ray diffraction patterns of the polycrystalline samples of $Na_{1.5}Eu_{8.5}(SiO_4)_6OF$, $NaEu_9(SiO_4)_6O_2$, $Gd_{9.34}(SiO_4)_6O_2$, and $Eu_{9.34}(SiO_4)_6O_2$ are included in the Supporting Information. This material is available free of charge via the Internet at http://pubs.acs.org.

■ AUTHOR INFORMATION

Corresponding Author

*E-mail: zurloye@mailbox.sc.edu. Phone: (803) 777-6916. Fax: (803) 777-8508.

Notes

The authors declare no competing financial interest.

■ ACKNOWLEDGMENTS

This research was supported by the National Science Foundation through grant DMR-1301757.

■ REFERENCES

(1) Masubuchi, Y.; Higuchi, M.; Takeda, T.; Kikkawa, S. *Solid State Ionics* **2006**, *177*, 263−268.
(2) Hopkins, R. H.; Melamed, N. T.; Henningsen, T.; Roland, G. W. *J. Cryst. Growth* **1971**, *10*, 218−222.
(3) Ferdov, S.; Sa Ferreira, R.; Lin, Z. *Chem. Mater.* **2006**, *18*, 5958−5964.
(4) Pasero, M.; Kampf, A. R.; Ferraris, C.; Pekov, I. V.; Rakovan, J.; White, T. J. *Eur. J. Mineral* **2010**, *22*, 163−179.
(5) Henderson, C. M. B.; Bell, A. M. T.; Charnock, J. M.; Knight, K. S.; Wendlandt, R. F.; Plant, D. A.; Harrison, W. J. *Mineral Mag.* **2009**, *73*, 433−455.
(6) Baikie, T.; Ahmad, Z.; Srinivasan, M.; Maignan, A.; Pramana, S. S.; White, T. J. *J. Solid State Chem.* **2007**, *180*, 1538−1546.
(7) Takahashi, M.; Uematsu, K.; Ye, Z.-G.; Sato, M. *J. Solid State Chem.* **1998**, *139*, 304−309.
(8) Latshaw, A. M.; Smith, M. D.; zur Loye, H.-C. *Solid State Sci.* **2014**, *35*, 28−32.
(9) Mugavero, S. J., III; Bharathy, M.; McAlum, J.; zur Loye, H.-C. *Solid State Sci.* **2008**, *10*, 370−376.
(10) Leu, L.-C.; Thomas, S.; Sebastian, M. T.; Zdzieszynski, S.; Misture, S.; Ubic, R. *J. Am. Ceram. Soc.* **2011**, *94*, 2625−2632.
(11) Waychunas, G. A. *Rev. Mineral Geochem.* **2002**, *48*, 701−742.
(12) *SMART*, version 5.630; *SAINT+*, version 6.45; *SADABS*, version 2.10; Bruker Analytical X-ray Systems, Inc.: Madison, WI, 2003.
(13) Sheldrick, G. M. *Acta Crystallogr.* **2008**, *A64*, 112−122.
(14) Hübschle, C. B.; Sheldrick, G. M.; Bittrich, B. *J. Appl. Crystallogr.* **2011**, *44*, 1281−1284.
(15) Smolin, Y. I.; Shepelev, Y. F. *Izv. Akad. Nauk SSSR, Neorg. Mater.* **1969**, *5*, 1823−1825.
(16) Parthé, E.; Gelato, L. M. *Acta Crystallogr.* **1984**, *A40*, 169−183.
(17) Gelato, L. M.; Parthé, E. *J. Appl. Crystallogr.* **1987**, *20*, 139−143.
(18) Hu, S.-Z.; Parthé, E. *Chin. J. Struct. Chem.* **2004**, *23*, 1150−1160.
(19) Morrison, G.; zur Loye, H.-C. 2014, Submitted.
(20) Felsche, J. *J. Solid State Chem.* **1972**, *5*, 266−275.
(21) Bugaris, D. E.; zur Loye, H.-C. *Angew. Chem., Int. Ed.* **2012**, *51*, 2−34.
(22) White, T.; Ferraris, C.; Kim, J.; Madhavi, S. *Rev. Mineral Geochem.* **2005**, *57*, 307−401.
(23) Toumi, M.; Smiri-Dogguy, L.; Bulou, A. *Ann. Chim. Sci. Mater.* **2002**, *27*, 17−26.
(24) Shen, Y.; Tok, A.; Dong, Z. *J. Am. Ceram. Soc.* **2010**, *93*, 1176−1182.
(25) Schroeder, L. W.; Mathew, M. *J. Solid State Chem.* **1978**, *26*, 383−387.
(26) Chiu, Y.-C.; Liu, W.-R.; Yeh, Y.-T.; Jang, S.-M.; Chen, T.-M. *J. Chem. Chem. Eng.* **2011**, *5*, 841−846.
(27) Lü, W.; Jia, Y.; Lv, W.; Zhao, Q.; You, H. *New J. Chem.* **2013**, *37*, 3701−3705.
(28) Nötzold, D. A. W. H. *Phys. Stat. Sol. (B)* **1998**, *207*, 271−282.
(29) An, T.; Baikie, T.; Wei, F.; Pramana, S. S.; Schreyer, M. K.; Piltz, R. O.; Shin, J. F.; Wei, J.; Slater, P. R.; White, T. J. *Chem. Mater.* **2013**, *25*, 1109−1120.

(30) Maisonneuve, V.; Leduc, E.; Bohnke, O.; Leblanc, M. *Chem. Mater.* **2004**, *16*, 5220−5222.
(31) White, T. J.; ZhiLi, D. *Acta Crystallogr.* **2003**, *B59*, 1−16.
(32) Lim, S. C.; Baikie, T.; Pramana, S. S.; Smith, R.; White, T. J. *J. Solid State Chem.* **2011**, *184*, 2978−2986.
(33) Wagner, C. D.; Riggs, W. M.; Davis, L. E.; Moulder, J. F. *Handbook of X-ray Photoelectron Spectroscopy*; Perkin-Elmer Corporation: Eden Prairie, MN, 1979; p 169.
(34) Blasse, G.; Grabmaier, B. C. *Luminescent Materials*; Springer-Verlag: New York, 1994.

dx.doi.org/10.1021/ic502185b | *Inorg. Chem.* 2015, 54, 876−884